Results in Surfaces and Interfaces 18 (2025) 100465

Contents lists available at ScienceDirect

Results in Surfaces and Interfaces

journal homepage: www.elsevier.com/locate/rsurfi

Ruthenium implantation for corrosion resistance: Using 2^k factorial design to determine significant implantation parameters

Fortunate Moyo [a,*], Josias van der Merwe [b,c], Daniel Wamwangi [b,d]

[a] School of Mechanical Engineering, North-West University, Private Bag X6001, 2520, Potchefstroom, South Africa
[b] Chemical and Metallurgical Engineering, University of the Witwatersrand, Private Bag, 2050, Johannesburg, South Africa
[c] DST-NRF Centre of Excellence in Strong Materials, University of the Witwatersrand, Private Bag P2, 2050, Johannesburg, South Africa
[d] School of Physics, University of the Witwatersrand, Private Bag, 2050, Johannesburg, South Africa

ARTICLE INFO

Keywords:
Stainless steel
Factorial design
Corrosion resistance
Ruthenium
Ion implantation

ABSTRACT

A 2^3 factorial design was used to study the effect of implantation energy (A), implantation dose (B), and surface roughness (C) on the corrosion resistance of ruthenium implanted AISI 304L stainless steel in 1 M sulfuric acid. Potentiodynamic polarization was used to determine corrosion rates of the samples, and a 3-way ANOVA test was used to calculate the effects of the independent variables and their interactions on the corrosion resistance of the ruthenium implanted stainless steel. It was shown that the interactive effects of implantation dose and surface roughness (BC), and of implantation energy and surface roughness (AC) are significant to the corrosion resistance of the ruthenium implanted stainless steel. In fact, the lowest corrosion rates were obtained with (1) high implantation dose and high surface roughness, and (2) low implantation energy and high surface roughness. XRD measurements done prior to corrosion exposure showed a 2.1–2.6% lattice expansion for surfaces with high roughness compared to 1.6–2.1% for polished surfaces, suggesting a higher surface concentration of ruthenium on stainless steel substrates with high surface roughness. The strong dependence of the implantation parameters and subsequently corrosion resistance of the 304L stainless steel on surface roughness is compelling. It suggests that roughening substrates prior to ion implantation for corrosion resistance could be more beneficial than polishing them as is common practice.

1. Introduction

Ruthenium has been shown to markedly improve the corrosion resistance of stainless steel alloys in reducing acidic environments (Potgieter and Brookes, 1995; Olubambi et al., 2009; Olaseinde et al., 2012; Sherif, 2012) such as those found in flotation, electrowinning and fuel cells. The improvement in corrosion resistance is due to cathodic modification brought about by Ru. Cathodic modification, a phenomenon first observed in 1911 (Monnartz, 1911) and later developed by Nikon Tomashov and co-workers (Tomashov, 1964), involves introducing active cathodes such as Ru into stainless steel. This lowers the stainless steel's hydrogen overvoltage, increases the exchange current density for H_2 evolution, and consequently shifts its corrosion potential into the passive region where the protective chromium (III) oxide is stable.

Although alloying with Ru has the potential to increase the tolerance of stainless steels in reducing acidic environments, even those with abrasive suspension (Wolff, 1999), the prohibitive cost of Ru limits commercialisation and widespread application of the corrosion protection technique. This has prompted research in thin anticorrosion Ru films, with films produced by electron beam vaporization, RF magnetron sputtering and pulsed electrodeposition (Potgieter et al., 1992; Moyo et al., 2016, 2018) showing considerable success. Thin Ru films undoubtably present an economical alternative to bulk alloying considered previously (Potgieter and Brookes, 1995; Olubambi et al., 2009; Olaseinde et al., 2012; Sherif, 2012). However, Ru is inherently brittle, and these films tend to spall severely and delaminate during corrosion exposure, putting to question their practical applicability and longevity.

Ion implantation, initially used for doping semiconductors, has generated considerable interest in corrosion studies (Abreu et al., 2002, 2008; Padhy et al., 2010; Cano et al., 2006; Tjong and Chu, 2007; Escalada et al., 2013). It is a low temperature technique that offers the ability to enrich subsurface regions of a metal with any element

* Corresponding author.
E-mail addresses: fortunate.moyo@nwu.ac.za (F. Moyo), Josias.VanDerMerwe@wits.ac.za (J. van der Merwe), daniel.wamwangi@wits.ac.za (D. Wamwangi).

https://doi.org/10.1016/j.rsurfi.2025.100465
Received 8 June 2024; Received in revised form 10 February 2025; Accepted 21 February 2025
Available online 22 February 2025

regardless of their miscibility. Surfaces produced by ion implantation have zero risk of cracking, buckling, spalling or delamination, as they do not have definable interfaces that could be subjected to mechanical weaknesses or interfacial corrosion (Dearnaley, 1978). In addition, implantation doses as low as 10^{15} to 10^{17} ions/cm^2 can impart appreciable corrosion resistance as demonstrated in numerous studies (Abreu et al., 2002, 2008; Padhy et al., 2010; Cano et al., 2006; Tjong and Chu, 2007) making the approach cost effective. Collectively, these factors make Ru implantation for corrosion resistance of stainless steel highly attractive and worth examination.

Metal ion implantation for improved corrosion resistance is largely understudied, with documented studies limited to implantation of stainless steels with titanium and cerium for improved corrosion resistance in sodium chloride and sodium hydroxide (Abreu et al., 2002; Escalada et al., 2013). Rarer still is the study on Ru implantation, with only one notable work by Tjong and Chu in 2007 (Tjong and Chu, 2007), which focused on Ru implantation of ferritic stainless steel for corrosion resistance in 0.5 M sulfuric acid. Despite the encouraging results, no similar study has been done since then, leaving a knowledge gap that requires empirical evidence to address.

A comprehensive understanding of Ru implantation for corrosion resistance of stainless steels must begin with a parametric study. The objective of this study, therefore, was to use 2^k factorial design to determine Ru implantation parameters beneficial to the corrosion resistance of AISI 304L stainless steel in 1 M H_2SO_4. Parameters studied were implantation energy, implantation dose and surface roughness, and corrosion performance was characterized using potentiodynamic polarization. In addition to reducing experimentation time and cost, 2^k factorial design can reveal parameters with interactive effects, which would be impossible with a one-factor-at a time experimental approach.

2. Materials and methods

2.1. Sample preparation

Samples measuring 20 × 20 × 6 mm were sectioned from a 304L stainless steel plate with 18.32% chromium and 8.2% nickel. One set of samples were wet ground using silicon carbide paper 120 grit to give an average surface roughness of ≈0.82 μm. Another set of samples were further ground using SiC paper of progressively finer grit, and eventually polished using 6 μm alumina paste to give an average surface roughness of ≈0.11 μm. Thereafter, all samples were cleaned ultrasonically in deionized water (>1 M Ω.cm) to dislodge any SiC or alumina particles, and then degreased with ethanol. The corrosion rate and corrosion potential (E_{corr}) of the as received 304L stainless steel in 1 M H_2SO_4 were 0.89 mm/y and −366 mV respectively.

The target used for ion implantation was prepared using a 99% pure Ru powder supplied by Anglo Platinum, South Africa. The powder was consolidated using spark plasma sintering at 1400 °C and 30 MPa as described by Angerer et al. (2009). The target was 20 mm in diameter and 2 mm thick. Ion implantation was carried out in a Varian 350D implanter at iThemba LABS North, South Africa. The implanter's energy and dose capacity ranged from 50 to 160 keV and 10^{12} to 10^{16} Ru/cm^2 respectively. Implantation was done at room temperature and 0° incidence angle.

To understand the effect of implantation energy on the distribution of Ru in the stainless steel substrate, the implantation process was simulated using SRIM-2008 in the full cascade mode and with 5000 ions. It should be noted that the Ru distribution obtained via this simulation was only an approximation. However, the results of the simulation were deemed sufficient for comparison purposes.

2.2. Design of experiments

A 2^3 factorial design was used for the 3 independent variables implantation energy, implantation dose, and surface roughness. These were studied at two levels; high (+) and low (−) as described in Table 1. Eight experiments were designed with the variables in Table 1 varied as described in Table 2. All experiments were randomized, and 5 samples were tested for each experiment in Table 2. A 3-way ANOVA test was used to calculate the effects of the variables in Table 1 and their interactions on the corrosion resistance of the Ru implanted stainless steel samples in 1 M H_2SO_4. The significance of the effects thus calculated was determined using a normal probability plot. In a normal probability plot, effects that do not fit reasonably well in a straight line are regarded significant, while those that fit in a straight line are normally distributed and are considered insignificant.

2.3. Materials characterisation

The quantities of Ru implanted into the 304L stainless steel samples could not be determined directly. However, it was expected that implanted Ru would increase interplanar spacing in the stainless steel lattice, and that the extent of increase would be directly proportional to the concentration of Ru introduced in the lattice, as observed previously on stainless steels implanted with nitrogen, molybdenum and silver (Mändl et al., 2005; Dudognon et al., 2008). Interplanar spacing is related to the Bragg angle, which can be measured by X-ray diffraction (XRD) with appreciable accuracy. A shift of an XRD peak to lower Bragg angles would suggest an increase in interplanar spacing. Although less than ideal, this approach was sufficient to allow for drawing sound conclusions. In this study, XRD measurements were done using a Bruker D2 Phaser with a LynxEye detector and Fe-filtered Co-Kα radiation. The XRD measurements were performed before corrosion exposure, and the data obtained was analyzed using Diffrac.Eva V3.2 software.

Potentiodynamic polarization was done in a 3-electrode cell consisting of the Ru implanted stainless steel sample as the working electrode, Ag/AgCl reference electrode and a large area graphite counter electrode. The tests were carried out in a Metrohm PGSTAT 302 Autolab interfaced with Nova 1.7 data acquisition software. Prior to polarization, the samples were held at OCP for 120s, and then polarized at a scan rate of 0.5 mV/s vs OCP. Corrosion rates were determined by the Stern-Geary method as described in ASTM G102. The corrosion tests were carried out in freshly prepared 1 M H_2SO_4 as widely done by previous researchers (Olubambi et al., 2009; Olaseinde et al., 2012; van der Merwe and Tharandt, 2015) on stainless steel alloys modified with Ru. All tests were done under natural aeration and static conditions with the temperature controlled by a water bath at 25 ± 1 °C.

3. Results

3.1. SRIM simulation

Fig. 1 and Table 3 show that implantation depth increased with increase in implantation energy. The depth of the Ru peak concentration was ≈13 nm at 50 keV and increased to almost 34 nm at 160 keV. The skewness at 50 keV was more positive, indicating that the implanted Ru was closer to the surface than at 160 keV and therefore more readily available for corrosion processes.

Notably, Ru distribution at 160 keV had a long tail (Fig. 1) consistent with marked channeling. Channeling occurs when the implanted ions travel between the atoms and crystallographic plans of the substrate.

Table 1
Factors and experimental levels used for the 2^3 factorial design of experiments.

Factor	Parameter	Low (−)	High (+)
A	Energy (keV)	50	160
B	Dose (Ru/cm^2)	10^{12}	10^{14}
C	Surface roughness	Polished[a]	Rough[b]

[a] Ra ≈0.11 μm.
[b] Ra ≈0.82 μm.

Table 2
Experimental levels used for the 8 experiments. Five samples were tested for each experiment.

Experiment number	Experimental level		
	A	B	C
1	+	−	+
2	+	+	−
3	−	+	−
4	+	+	+
5	+	−	−
6	−	−	+
7	−	−	−
8	−	+	+

The consequence of channeling is implantation depths larger than the predicted distribution. Ru distribution at 50 keV had a much shorter tail pointing to less channeling and a higher likelihood for the Ru ions stopping at shallow depths.

The lateral straggle was larger at 160 keV than at 50 keV (Table 3); it was in fact 149% wider. This suggests that the Ru ions implanted at the higher energy interacted more with the atoms of the 304L stainless steel substrate. The consequence of this is a large volume of damage due to the knock-on effect of implanted Ru ions, which could be detrimental to corrosion resistance of the implanted stainless steel.

3.2. XRD analysis

XRD diffractograms for Ru implanted 304L stainless steel shown in Fig. 2(a) are identical to those for unmodified 304L stainless steel. The absence of Ru peaks suggests that the amounts of Ru implanted into the stainless steel substrates were lower than 4 vol%, the detection limit of the D2 Phaser used in this study. In all cases studied (Table 2), there was a shift of the (111) and (200) peaks to Bragg angles lower than 51.97° and 60.64° measured on as received 304L stainless steel. The shift in the Bragg angle suggests an increase in interplanar spacing consistent with volumetric expansion of the 304L stainless steel lattice due to the implanted Ru.

As can be seen in Fig. 2(b), and except for one case, Ru implantation into the rough stainless steel samples resulted in larger shifts in the Bragg angle. Angular shift of the (111) peak was between 2.1 and 2.6% for the rough samples, while the shift of the same peak for the polished samples ranged from 1.6 to 2.2%. These observations seem to imply that more Ru was implanted into the subsurface of the rough samples leading to larger lattice expansion. The largest shift, a 2.6% decrease in Bragg angle, was associated with the rough samples implanted at low energy and high dose. This set of samples would be expected to exhibit low corrosion rates in 1 M H_2SO_4, consistent with the expectation that the corrosion resistance of Ru modified stainless steels increases with increase in Ru concentration (Olubambi et al., 2009; Potgieter et al., 1995; Sherif, 2011).

At high implantation energy and dose (Fig. 2(b)) the effect of surface roughness on Bragg angle was indistinguishable. The 2θ position of the (111) peak as measured on the rough and the polished samples was 50.8 and 50.9° respectively. This could be due to the channeling reported in Fig. 1 at high implantation energy and is consistent with the expectation of a deeper Ru distribution in these samples.

3.3. Corrosion characterisation

The presence of Ru shifted E_{corr} of 304L stainless steel to nobler values as illustrated in Fig. 3(a). However, the effect of Ru implantation on E_{corr} was rather slight, given that the E_{corr} of as received 304L stainless steels was −366 mV. Slight increases in E_{corr} values after Ru additions to stainless steel were also noted by other researchers (Olubambi et al., 2009; Sherif, 2011) although in both cases this was accompanied by a marked decrease in corrosion current density and hence corrosion rates. In this work, the biggest change in E_{corr} was observed on the rough samples prepared at 50 keV and 10^{14} Ru/cm^2; E_{corr} increased to ≈ −263 mV.

From Fig. 3(b), the highest corrosion rates were obtained on the rough samples implanted at low dose (10^{12} Ru/cm^2) and high energy (160 keV). Corrosion rates for this set of samples were as high as 1.4 mm/y and averaged 0.89 mm/y. This is the same as the corrosion rate of unmodified 304L stainless steel, which was ≈0.89 mm/y; meaning that Ru implantation at high energy and low dose did not improve corrosion

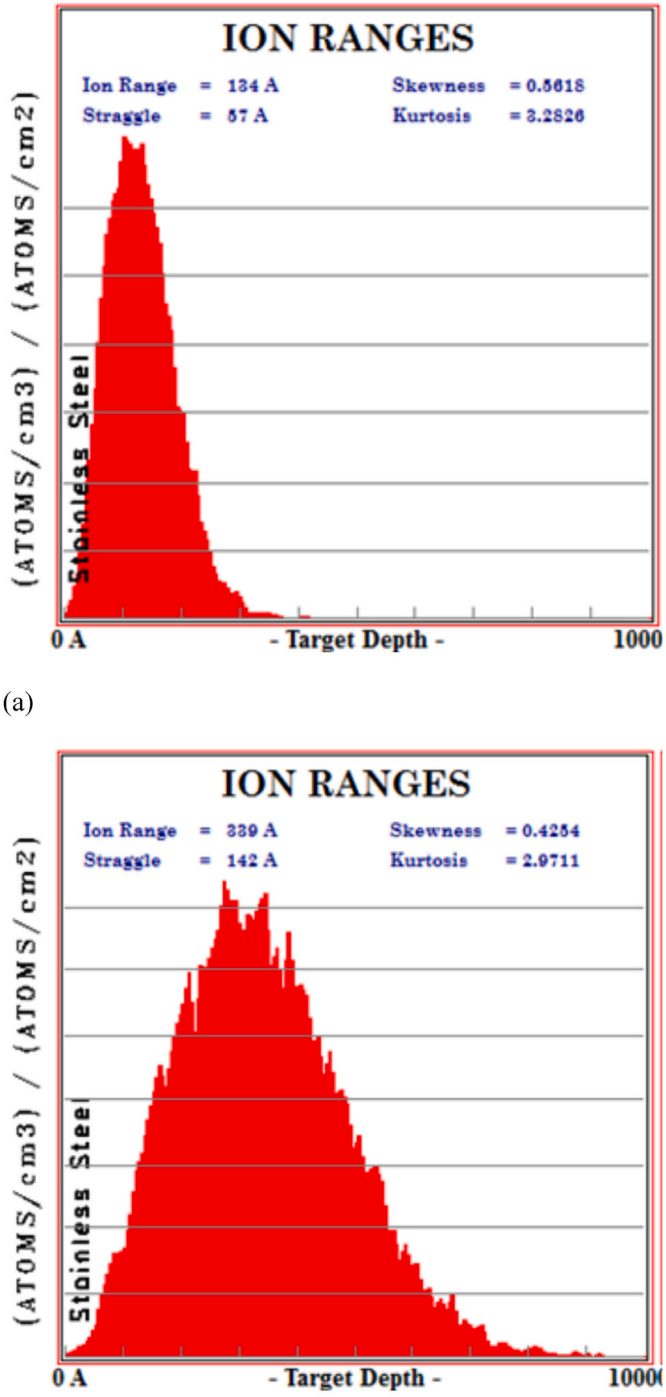

Fig. 1. Distribution of Ru implanted in 304L stainless steel as simulated as (a) 50 keV, and (b) 160 keV. Angle of incidence = 0°.

Table 3
Effect of implantation energy on Ru distribution in 304L stainless steel as determined by SRIM simulation.

Parameter	Implantation energy (keV)	
	50	160
Ion range (nm)	13.4	33.9
Lateral straggle (nm)	5.7	14.2
Skewness	0.5618	0.4254
Kurtosis	3.2826	2.9711

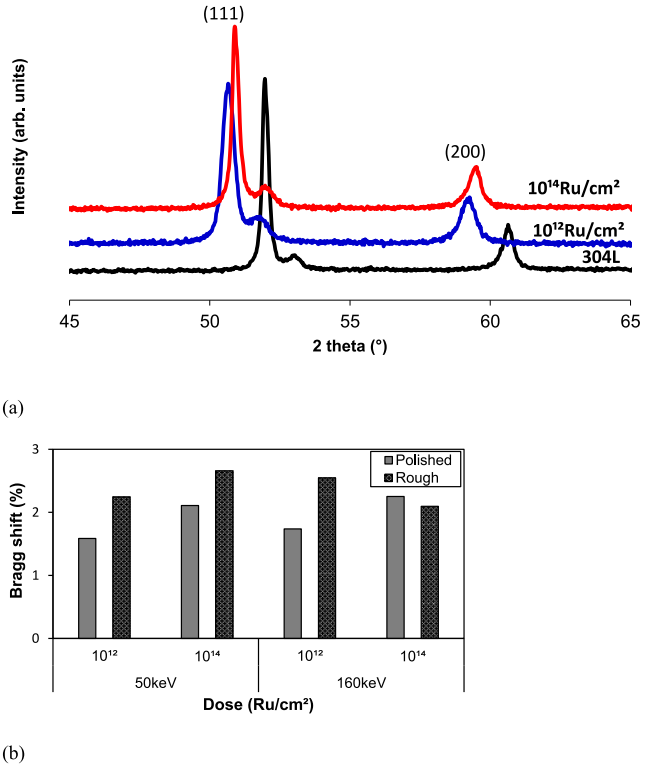

Fig. 2. (a) Typical XRD diffractograms for Ru implanted 304L stainless steel, and (b) effects of implantation dose, implantation energy, and surface roughness on the Bragg angle of the (111) peak. Three samples were tested per condition.

resistance at all.

The least average corrosion rate recorded was 0.062 mm/y and was measured on rough samples prepared at low energy and high dose (Fig. 3 (b)). For this set of samples, corrosion rates ranged from 0.014 to 0.183 mm/y, consistent with protection efficiency (Sherif, 2011) of at least 79%. At first glance this observation is atypical since rough surfaces are usually associated with high corrosion rates (Melchers and Jeffrey, 2004; Li and Li, 2006). However, the results in Fig. 3(b) are consistent with the expectations that (1) at low implantation energy, Ru would be distributed closer to the surface (Fig. 1 and Table 3) and more accessible for corrosion processes; and (2) this set of samples experienced the largest Bragg angle shift in Fig. 2(b) and supposedly had the largest subsurface concentration of Ru.

Interestingly, corrosion rates of polished samples increased with increase in implantation dose regardless of energy. This response was contrary to expectation that higher doses would cause improved corrosion resistance as demonstrated previously (Padhy et al., 2010). For rough samples though, corrosion rates decreased with increase in dose, which was expected. This peculiar trend suggests that surface roughness had a marked effect on the corrosion resistance of the Ru implanted stainless steel.

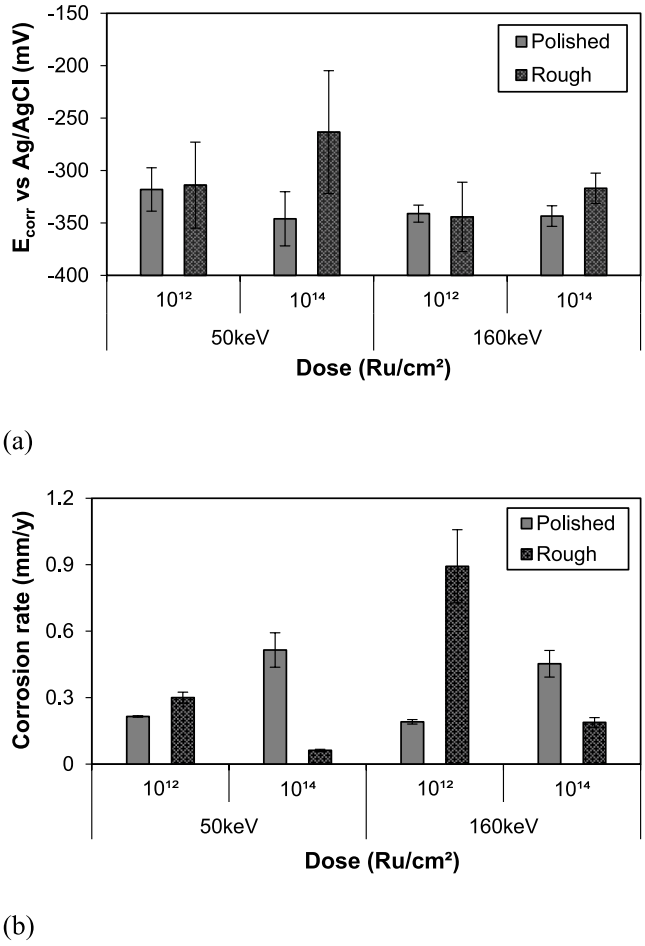

Fig. 3. Influence of implantation energy, implantation dose, and surface roughness on (a) E_{corr}, and (b) corrosion rate of Ru implanted 304L stainless steel in 1 M H_2SO_4.

3.4. Significant parameters

The normal probability plot in Fig. 4 shows that the effects of surface roughness (C) and implantation dose (B) (Table 2) as well as the interactions AB and ABC approximately lie in a straight line and were therefore normally distributed and insignificant. The revelation that dose was insignificant to the corrosion resistance of Ru implanted 304L stainless steel was quite surprising. It was natural to expect that Ru concentration would have a significant effect on the corrosion resistance

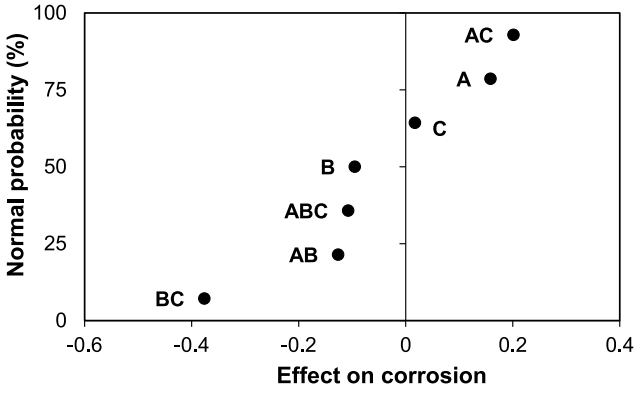

Fig. 4. Normal probability plot for the main factors A-implantation energy, B-implantation dose, and C- surface roughness, and their interactions.

of the Ru implanted stainless steel as demonstrated by other researchers in similar corrosion control systems (Olubambi et al., 2009; Padhy et al., 2010; Potgieter et al., 1995; Sherif, 2011).

Parameters that seemed significant to the corrosion resistance of Ru implanted 304L stainless steel were energy (A) (Table 2), and the interaction of energy and surface roughness (AC) and that of dose and surface roughness (BC). As can be seen in Fig. 4, the effects of these parameters did not fit reasonably well on a straight line. Interaction of effects takes precedence over effects of individual factors, i.e., the interactions AC and BC were more important than the factor A. Therefore, further analysis was focused on these interactions only.

Interactions AC and BC were disordinal as can be seen by the intersections of the graphs in Fig. 5. This indicates that the effects of energy and dose on the corrosion resistance of Ru implanted 304L stainless steel were strongly dependent on surface roughness of the substrate pre ion implantation.

In Fig. 5(a), increasing both implantation energy and surface roughness had the effect of increasing the corrosion rates of the Ru implanted stainless steel. The results are consistent with the expectation that (1) at high implantation energy, Ru distribution was deeper in the subsurface (Fig. 1 and Table 3) and less available for corrosion processes; (2) high implantation energies are associated with greater damage as alluded to in Fig. 1; and (3) rough surfaces are generally prone to high corrosion rates. On the other hand, increasing implantation energy on polished samples caused a decrease in corrosion rate of the Ru implanted stainless steel in 1 M H_2SO_4. The decrease was however marginal, ≈11%, compared to ≈66% when decreasing implantation energy on rough samples (Fig. 5(a)).

Simultaneously increasing dose and surface roughness also led to low corrosion rates as can be seen in Fig. 5 (b). Increasing implantation dose from 10^{12} to 10^{14} Ru/cm^2 on rough surfaces increased corrosion resistance by a factor >4.5. While it was expected that increasing implantation dose would improve corrosion resistance, a similar effect was not expected with increasing surface roughness. On polished surfaces, increasing implantation dose had the opposite effect: increasing dose on these surface increased corrosion rates by as much as 138%.

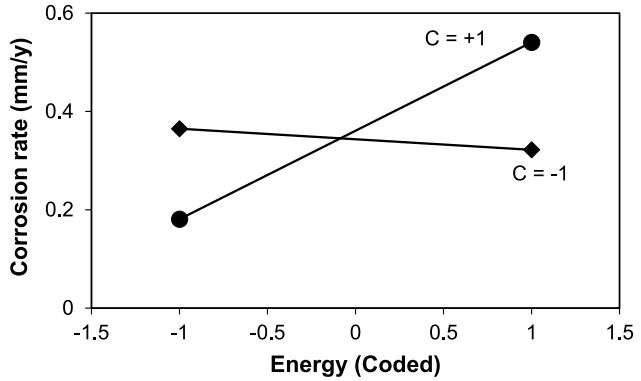

(a)

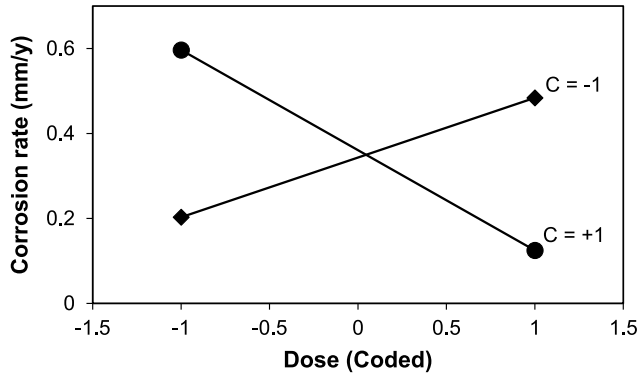

(b)

Fig. 5. Interaction graphs for the effects of (a) implantation energy and surface roughness (AC), and (b) implantation dose and surface roughness (BC) on the corrosion rate of Ru implanted 304L stainless steel in 1 M H_2SO_4. C = +1 means high surface roughness, and C = −1 means low surface roughness.

4. Discussion

In most of the cases studied, 7 of the 8 experiments detailed in Table 2, introducing Ru to 304L stainless steel by ion implantation improved corrosion resistance in 1 M H_2SO_4 by between 42 and 93%. This confirms the potential of the technique as an anti-corrosion method and is consistent with the results obtained by Tjong and Chu (2007) on Ru implanted Fe–24Cr ferritic stainless steel in 0.5 M H_2SO_4.

During corrosion exposure of cathodically modified alloys, it is postulated that selective dissolution of the base alloy leads to surface enrichment of the active cathodes like Ru (Pickering, 1983), and the rate of surface enrichment is a function of the concentration of the active cathode in the alloy. Hence for samples implanted at 160 keV and having a deeper distribution of Ru (Fig. 1 and Table 3), the rate of surface enrichment would be low, and the effectiveness of cathodic modification reduced. This could explain the decrease in corrosion resistance associated with high implantation energy.

Interestingly, increasing implantation energy from 50 to 160 keV had a similar and marginal effect on the corrosion rate of polished Ru implanted stainless steel regardless of implantation dose (Fig. 3(b)). At 10^{12} Ru/cm^2, increasing implantation energy caused ≈11% decrease in corrosion rate and ≈12% at 10^{14} Ru/cm^2. This seems to suggest that the depth of Ru in these samples, and hence its availability for the corrosion process was the same irrespective of implantation energy. A similar trend was not observed on the rough samples.

One of the challenges associated with ion implantation of polycrystalline substrates like 304L stainless steel is channeling. Channeling results in a deeper than predicted distribution of the implanted element and reduces its concentration near the surface. In Fig. 1, while channeling was significant at 160 keV, it was just as likely at 50 keV albeit to a lesser extent. It is possible therefore that the actual ion range for the polished 304L stainless steel was deeper than 13 nm predicted by SRIM simulation in Fig. 1 and Table 3.

Amorphization of the substrate can significantly reduce channeling, and one of the simplest methods of achieving a nearly amorphous surface is through surface roughening. Increasing surface roughness from 0.11 to 0.82 μm could have introduced disorder and heterogeneity in the arrangement of crystallographic planes in the subsurface of the 304L stainless steel substrate. A possible consequence of this is a decrease in the stopping distance of the implanted Ru ions, such that the actual ion range for the rough 304L stainless steel samples was shallower than that predicted by the SRIM simulation in Fig. 1 and Table 3. This could explain the decrease in corrosion rates with increase in ion implantation dose observed in Fig. 4(b), and the larger shift in the (111) Bragg angle in Fig. 2(b).

In all the cases studied, Ru implantation shifted the Bragg angles of the (111) peak to lower values (Fig. 2), indicative of compressive stresses in the Ru implanted stainless steel samples. Compressive stresses in ion implantation are mainly due to interstitial atoms (Paine and Speriosu, 1987) causing volumetric expansion of the substrate lattice. Schubert et al. (1984) showed that the expansion of a niobium crystal lattice was linearly proportional to the concentration of nitrogen implanted in it. Similar results are reported in Fig. 2, where in most cases, increasing implantation dose from 10^{12} to 10^{14} Ru/cm^2 increased the Bragg angle shift.

The quantities of Ru implanted in the 304L stainless steel were too small, <4 vol%, to be successfully detected by techniques such as energy dispersion spectroscopy, auger electron spectroscopy, and transmission electron microscopy, results of which are not shown here but are available upon request. It is however plausible to conclude from the XRD results in Fig. 2(b) that there were larger concentrations of Ru implanted in the subsurface of the rough samples than in the polished ones. This is consistent with the supposition that amorphization of the stainless steel surfaces by roughening reduced the stopping range of the Ru ions, led to shallower implantation depths, and increased the availability of the Ru for effective cathodic modification. The lower corrosion rates reported on most of these samples in Fig. 3(b) corroborate this. These results are very important since it is common practice to polish samples prior to ion implantation for corrosion application (Abreu et al., 2002, 2008; Padhy et al., 2010; Tjong and Chu, 2007).

5. Conclusion

The effect of three Ru implantation parameters, implantation energy, implantation dose and surface roughness, on the corrosion rate of 304L stainless steel in 1 M H_2SO_4 was studied using 2^k factorial design. Contrary to expectation, the best corrosion performance was observed on the rough surface samples with average corrosion rates as low as 0.062 mm/y compared to 0.191 mm/y the lowest average reported on the polished samples. In fact, low corrosion rates were achievable under two conditions: (1) low implantation energy and high surface roughness, and (2) high implantation dose and high surface roughness. Polishing the stainless steel samples, a common practice, was not beneficial to the corrosion resistance of the implanted alloy in H_2SO_4.

This preliminary work presents a strong and compelling dependence of surface roughness on the effects of implantation dose and implantation energy on corrosion resistance of Ru implanted stainless steel, a previously undocumented observation. Future analysis is required to determine the underlying cause of this behavior, and to optimize the interactions parameters for maximum corrosion resistance. In addition, the distribution of the implanted Ru in the stainless steel substrates needs to be experimentally determined.

CRediT authorship contribution statement

Fortunate Moyo: Writing – review & editing, Writing – original draft, Methodology, Investigation, Formal analysis, Conceptualization. **Josias van der Merwe:** Writing – review & editing, Supervision, Resources, Project administration, Conceptualization. **Daniel Wamwangi:** Writing – review & editing, Supervision, Resources, Methodology.

Declaration of competing interest

The authors declare that they have no known competing financial interests or personal relationships that could have appeared to influence the work reported in this paper.

Acknowledgements

The support of DST-NRF Centre of Excellence in Strong Materials (CoE-SM) towards this research is hereby acknowledged. The Department of Science and Technology, and National Research Foundation, South Africa are thanked for financial support.

Appendix A. Supplementary data

Supplementary data to this article can be found online at https://doi.org/10.1016/j.rsurfi.2025.100465.

Data availability

Data will be made available on request.

References

Abreu, C.M., Cristóbal, M.J., Nóvoa, X.R., Pena, G., Pérez, M.C., 2002. Characterisation of the electrochemical behavior of cerium implanted stainless steels. Electrochim. Acta 47, 2215–2222. https://doi.org/10.1016/S0013-4686(02)00058-0.

Abreu, C.M., Cristóba, l M.J., Merino, P., Nóvoa, X.R., Pena, G., Pérez, M.C., 2008. Electrochemical behavior of an AISI 304L stainless steel implanted with nitrogen. Electrochim. Acta 53, 6000–6007. https://doi.org/10.1016/j.electacta.2008.03.064.

Angerer, P., Neubauer, E., Yu, L.G., Khor, K.A., 2009. Determination of the residual stress depth profile of uniaxial compacted ruthenium powder samples by x-ray diffraction. Int. J. Refract. Met. Mater. 27, 1004–1008. https://doi.org/10.1016/j.ijrmhm.2009.07.006.

Cano, E., Martínez, L., Simancas, J., Pérez-Trujillo, F.J., Gómez, C., Bastidas, J.M., 2006. Influence of N, Ar and Si ion implantation on the passive layer and corrosion behavior of AISI 304 and 430 stainless steels. Surf. Coat. Technol. 200, 5123–5131. https://doi.org/10.1016/j.surfcoat.2005.05.029.

Dearnaley, G., 1978. Ion implantation for improved resistance to wear and corrosion. Int. J. Mater. Eng. 1 (1), 28–41. https://doi.org/10.1016/0141-5530(78)90005-5.

Dudognon, J., Vayer, M., Pineau, A., Erre, R., 2008. Mo and Ag ion implantation in austenitic, ferritic and duplex stainless steels: a comparative study. Surf. Coat. Technol. 203, 180–185. https://doi.org/10.1016/j.surfcoat.2008.08.069.

Escalada, L., Lutz, J., Brühl, S.P., Fazoio, M., Márquez, A., Mändl, S., Manova, D., Simison, S.N., 2013. Microstructure and corrosion behaviour of AISI 36L duplex treated by means of ion nitriding and plasma based on implantation and deposition. Surf. Coat. Technol. 223, 41–46.

Li, W., Li, D.Y., 2006. Influence of surface morphology on corrosion and electronic behavior. Acta Mater. 54, 445–452. https://doi.org/10.1016/j.actamat.2005.09.017.

Mändl, S., Manova, D., Neumann, H., Pham, M.T., Ritcher, E., Rauscheubach, B., 2005. Correlation between PIII nitriding parameters and corrosion behavior of austenitic stainless steels. Surf. Coat. Technol. 200, 104–108. https://doi.org/10.1016/j.surfcoat.2005.02.084.

Melchers, R.E., Jeffrey, R., 2004. Surface roughness effect on marine immersion corrosion of mild steel. Corrosion 60 (7), 697–703. https://doi.org/10.5006/1.3287847.

Monnartz, P., 1911. Iron-chromium alloys with special consideration of resistance to acids. Metallurgie (Halle) 7 (8), 161–176.

Moyo, F., van der Merwe, J.W., Wamwangi, D., 2016. Corrosion performance of pulse plated ruthenium: dependence on pulse-off time. Surf. Coat. Technol. 307, 971–977. https://doi.org/10.1016/j.surfcoat.2016.10.016.

Moyo, F., van der Merwe, J.W., Wamwangi, D., 2018. Enhanced adhesion of anticorrosion ruthenium films deposited by RF sputtering on 304L stainless steel. Surf. Coat. Technol. 438, 128381. https://doi.org/10.1016/j.surfcoat.2022.128381.

Olaseinde, O.A., van der Merwe, J.W., Cornish, L.A., Chown, L.H., Olubambi, P.A., 2012. Electrochemical studies of Fe-12Cr-1Ni duplex stainless steel with 0.5 wt% ruthenium at different temperatures. J. South. Afri. Inst. Min. Metall. 7A, 535–538.

Olubambi, P.A., Potgieter, J.H., Cornish, L., 2009. Corrosion behavior of super ferritic stainless steels cathodically modified with minor additions of ruthenium in sulphuric and hydrochloric acids. Mater. Des. 30, 1451–1457. https://doi.org/10.1016/j.matdes.2008.08.019.

Padhy, N., Ningshen, S., Panigrahi, B.K., Mudali, K., 2010. Corrosion behavior of nitrogen ion implanted AISI type 304L stainless steel in nitric acid medium. Corros. Sci. 52, 104–112. https://doi.org/10.1016/j.corsci.2009.08.042.

Paine, B.M., Speriosu, V.S., 1987. Nonlinear strain effects in ion-implanted GaAs. J. Appl. Phys. 62 (5), 1704–1709. https://doi.org/10.1063/1.339596.

Pickering, H.W., 1983. Characteristic features of alloy polarization curves. Corros. Sci. 23 (10), 1107–1120.

Potgieter, J.H., Brookes, H.C., 1995. Corrosion behavior of a high chromium duplex stainless steel with minor additions of ruthenium in sulphuric acid. Corrosion 51 (4), 312–320. https://doi.org/10.5006/1.3293596.

Potgieter, J.H., Wentzel, E., Myburg, G., 1992. Effects of vapor deposited and bulk alloyed ruthenium of corrosion resistance of a duplex stainless steel in sulphuric acid. Surf. Eng. 8 (4), 289–291. https://doi.org/10.1179/sur.1992.8.4.289.

Potgieter, J.H., Ellis, P., van Bennekom, A., 1995. Investigation of the active dissolution behavior of a 22% chromium duplex stainless steel with small ruthenium additions in sulphuric acid. ISIJ Int. 35 (2), 197–202. https://doi.org/10.2355/isijinternational.35.197.

Schubert, U., Metzger, H., Peisl, J., 1984. Diffuse x-ray scattering from interstitial nitrogen in niobium: I. Haung diffuse scattering. J. Phys. F: Met. Phys. 14, 2457–2466. https://doi.org/10.1088/0305-4608/14/11/004.

Sherif, E.M., 2011. Corrosion behavior of duplex stainless steel alloy cathodically modified with minor ruthenium additions in concentrated sulfuric acid solutions. Int. J. Electrochem. Sci. 6, 2284–2298. https://doi.org/10.1016/S1452-3981(23)18184-3.

Sherif, E.M., 2012. Corrosion of duplex stainless steel alloy 2209 in acidic and neutral chloride solutions and its passivation by ruthenium as an alloying element. Int. J. Electrochem. Sci. 2, 2374–2388. https://doi.org/10.1016/S1452-3981(23)13886-7.

Tjong, S.C., Chu, P.K., 2007. Corrosion properties of Fe-24Cr stainless alloy modified by plasma immersion ion implantation on 0.5 M sulfuric acid solution. Surf. Coat. Technol. 201, 6781–6784. https://doi.org/10.1016/j.surfcoat.2006.09.049.

Tomashov, N.D., 1964. Passivity and corrosion resistance of metal systems. Corros. Sci. 4, 315–334.
van der Merwe, J., Tharandt, D., 2015. Corrosion resistance of laser-cladded 304L stainless steel enriched with ruthenium additions exposed to sulphuric acid and sodium chloride media. J. South. Afri. Inst. Min. Metall. 115, 499–505.
Wolff, I.M., 1999. New applications for ruthenium. South Afr. J. Sci. 95, 539–542 (November/December).